Polymer 50 (2009) 936–944

Contents lists available at ScienceDirect

Polymer

journal homepage: www.elsevier.com/locate/polymer

# Structure–property relationship of thermotropic liquid-crystalline vinyl polymers containing no traditional mesogen

Yan Guan, Xiaofang Chen, Zhihao Shen, Xinhua Wan*, Qifeng Zhou**

*Beijing National Laboratory for Molecular Sciences, Key Laboratory of Polymer Chemistry and Physics of Ministry of Education, College of Chemistry and Molecular Engineering, Peking University, 202 Cheng Fu Road, Beijing 100871, China*

ARTICLE INFO

*Article history:*
Received 10 September 2008
Received in revised form
15 November 2008
Accepted 1 December 2008
Available online 9 December 2008

*Keywords:*
Hexagonal columnar mesophase ($\Phi_H$)
Thermotropic liquid-crystalline property
Liquid-crystalline polymer

ABSTRACT

A series of non-mesogenic vinyl monomers, 2,5-bis(alkoxycarbonyl)styrene, were synthesized and polymerized via free radical polymerization. The alkoxy groups were systematically varied to investigate the effects of their size and architecture on the thermotropic liquid-crystalline properties of the resultant polymers. Although no traditional mesogen was present in the macromolecular structure, all the polymers revealed stable hexagonal columnar liquid-crystalline phase at the temperatures well above their glass transitions when the molecular weights were high enough, as evidenced by a combinatory analysis of differential scanning calorimetry, polarized light microscopy, and one- and two-dimensional wide-angle X-ray diffraction techniques. For the polymers containing five carbon atoms in the alkoxy terminals, the temperatures of glass transition and mesophase formation decreased and the *d*-spacing value of mesophase increased as the methyl substituent moved away from the connecting phenyl ring. Increasing the number of methyl group or the size of the substituent had the same effect. In the case of polymers with Y-shaped alkoxy terminals, the larger the side groups, the lower the glass-transition temperature and mesophase formation temperature and the larger the *d*-spacing value of mesomorphic structure.


## 1. Introduction

Generally, a polymer backbone, a mesogenic unit, and a flexible spacer that bridges the mesogenic unit and the polymer backbone comprise a side-chain liquid-crystalline polymer (SC-LCP) [1]. On the basis of the way in which mesogens are connected to the polymer backbones, SC-LCPs can be categorized into either "side-end-fixed" or "side-on-fixed" type [2–4]. According to Finkelmann et al. [5], the flexible spacer inserted between main chain and mesogenic unit is indispensable in order for a SC-LCP to achieve liquid-crystalline (LC) phase since it decouples the interaction of side chain and polymer backbone, which disrupts the ordered packing of the side mesogens. For the last twenty years, we have been working on a unique "side-on-fixed" SC-LCPs, named mesogen-jacketed liquid-crystalline polymers (MJLCPs) [6]. Unlike conventional "side-end-fixed" or "side-on-fixed" type SC-LCPs, mesogenic units are laterally attached to the main chain via only one covalent C–C bond or a very short spacer in MJLCPs [7–9]. Due to the strong coupling between the polymer main chain and the highly crowded, rigid, and bulky side groups, the macromolecules have to take an extended and stiffened conformation and order into mesophases as a whole as in main-chain LCPs [10], that is, an orientational packing of the supramolecular cylinder, the periphery of which is the high population of rigid side groups. This concept has been supported by studies of small-angle neutron scattering [11–15] and X-ray diffraction [16,17]. Additional evidences come from the observation of shear-induced banded textures [18,19] and a large persistent length value in solution [20]. The vast majority of MJLCPs synthesized by a number of research groups to date are mainly based on poly{2,5-bis[(4-alkoxybenzoyl)oxy]styrene} [8,21–24], poly[2,5-bis(4-alkoxybenzamido)styrene] [25], poly{2,5-bis[(4-alkoxyphenyl)oxycarbonyl]styrene} [26–31,40], poly[2,5-bis(alkoxycarbonyl)styrene] [10,39] and poly[2,5-bis(4-alkoxyphenyl)styrene] [32–36]. A columnar nematic phase ($\Phi_N$) is the most often observed phase structure in these MJLCPs [37,38]. Higher ordered liquid-crystalline (LC) structures, such as hexatic columnar nematic ($\Phi_{HN}$), two-dimensional hexagonal columnar phases (2D $\Phi_H$) and columnar rectangular phases, have also been observed [10,38–41]. Moreover, smectic A ($S_A$) and smectic C ($S_C$) phases have also been found in laterally attached side-chain LC polymers [42–47].

Our recent results indicate that such a molecular design strategy is very useful in building LCPs containing no traditional mesogen.

* Corresponding author. Tel.: +86 10 6275 4187; fax: +86 10 6275 1708.
** Corresponding author.
*E-mail addresses:* xhwan@pku.edu.cn (X. Wan), qfzhou@pku.edu.cn (Q. Zhou).

0032-3861/$ – see front matter © 2008 Elsevier Ltd. All rights reserved.
doi:10.1016/j.polymer.2008.12.002

For example, poly[di(4-heptyl) vinylterephthalate] [10] generates a supramolecular hexagonal columnar LC phase on a nanometer length scale by the self-assembly of non-mesogenic templates, which have only one phenylene group connected with two double-swallow tailed 4-heptyl (Y-shaped) groups via an ester linkage and is jacketed onto the backbone at every second carbon atom. Moreover, it has been found that the length of alkyl tail in a series of poly[di(alkyl)vinylterephthalates] has exerted a significant influence on the LC behaviors [39]. To form two-dimensional long-range ordered structure, the substituted ester groups at the 2- and 5-position of the phenyl ring laterally attached to the backbone should be in the range of propyl to hexyl. Other LCPs having no classical mesogen include polyphosphazenes [48–51] and poly(di-*n*-alkylsiloxane)s reported by Molenberg et al. [52–56]. However, the effects of size and architecture of terminals in the flexible side groups on the phase structures and transitions of such novel liquid-crystalline polymers have not been very clear and have not been investigated in a systematic manner.

In this work, we report synthesis and characterization of a series of non-mesogenic vinyl monomers, 2,5-bis(alkoxycarbonyl)styrene, along with their corresponding homopolymers. These polymers can be divided into two types. The first has alkoxy terminals containing five carbon atoms and substituted with methyl groups at different position, while the second has Y-shaped alkoxy terminals with different size. The structures of the monomers and the corresponding polymers and their abbreviations are depicted in Scheme 1. As evidenced by the results of differential scanning calorimetry (DSC), polarized light microscopy (PLM), and wide-angle X-ray diffraction (WAXD), all the polymers show stable 2D $\Phi_H$ liquid-crystalline phase and the subtle structural change leads to a remarkable impact on the glass-transition temperature, the temperature of mesophase formation, and the size of the mesomorphic structure.

## 2. Experimental section

### 2.1. Materials

Triphenylphosphine ($PPh_3$; 99%; Acros), ethyl 2-bromoisobutyrate (EBiB; 99%; Acros), and *N*,*N*,*N*′,*N*′,*N*″-pentamethyldiethylenetriamine (PMDETA; 99%; Aldrich) were used as received. All alcohols (analytical reagent; Beijing Chemical Co.) were purified by drying over $CaH_2$ and distillation. Pyridine (analytical reagent; Beijing Chemical Reagents Co.) was refluxed over KOH for at least 48 h and distilled out just before use. *N*,*N*-Dimethylformamide (DMF; analytical reagent; Beijing Chemical Reagents Co.) was refluxed over KOH for at least 6 h and distilled out just before use. Tetrahydrofuran (THF; analytical reagent; Beijing Chemical Reagents Co.) was refluxed over sodium under an argon atmosphere and distilled out before use. THF (HPLC grade; Fisher Chemical Co.) was directly used in the gel permeation chromatography (GPC) and laser light scattering measurements.

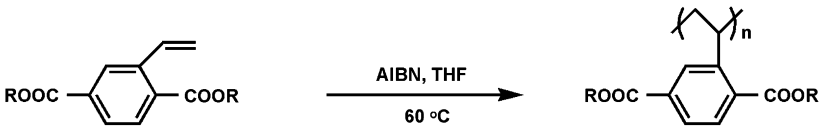


| R | Monomer | Polymer |
|---|---|---|
| 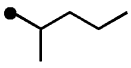 | C5-1M | PC5-1M |
| 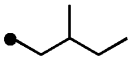 | C5-2M | PC5-2M |
| 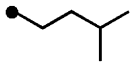 | C5-3M | PC5-3M |
|  | C5-1,2M | PC5-1,2M |
|  | C3-1M | PC3-1M |
| 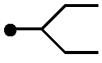 | C5-1E | PC5-1E |
| 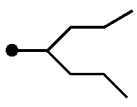 | C7-1P | PC7-1P |

**Scheme 1.** Radical polymerization of 2,5-bis(alkoxycarbonyl)styrene. ●: the site connecting to oxygen atom.

2,2′-Azobis(isobutyronitrile) (AIBN; 95%; Beijing Chemical Co.) was purified by recrystallization from ethanol (analytical reagent; Beijing Chemical Co.). Cuprous bromide (CuBr; 98%; Aldrich) was purified by stirring overnight in acetic acid. After filtration, it was washed with ethanol and ether and then dried under vacuum. Other reagents and solvents were purchased from Beijing Chemical Reagents Co. and used as received unless otherwise specified.

*2.1.1. Synthesis of the monomers*

*2.1.1.1. 2,5-Bis[(1-methyl butoxy)carbonyl]styrene (C5-1M).* Vinylterephthalic acid (0.77 g, 4.0 mmol) and triphenylphosphine (2.2 g, 8.4 mmol) were dissolved in 10 mL of dry pyridine to obtain solution A. Dry 2-pentanol (0.74 g, 8.4 mmol) and hexachloroethane (2.1 g, 8.8 mmol) were dissolved in 10 mL of dry pyridine to obtain solution B. Then the solution B was added dropwise into the solution A. The mixture was stirred at 60 °C for 5 h. After cooled to room temperature, the mixture was poured into dilute hydrochloric acid and extracted with chloroform for 3 times. The organic layer was combined and dried over anhydrous sodium sulfate. After evaporation of chloroform under vacuum, the residue was purified with silica gel column chromatography using dichloromethane as an eluent to get a colorless isotropic liquid with a yield of 60%. $^1$H NMR ($\delta$, ppm): 0.91–1.74 (m, 20H, –CH($CH_3$)$CH_2CH_2CH_3$), 5.17 (m, 2H, –CH<), 5.38–5.44 (dd, 1H, =$CH_2$), 5.71–5.80 (dd, 1H, =$CH_2$), 7.27–7.45 (q, 1H, =CH–), 7.84–8.23 (m, 3H, Ar–H). IR ($cm^{-1}$): 1408, 1466, 1484, 1564 (Ar–), 1719 (C=O), 2874 (–$CH_3$, $\nu_s$), 2935 (–$CH_2$–), 2961 (–$CH_3$, $\nu_{as}$), and 3090 (–CH=$CH_2$). MS (*m*/*e*): Calcd. 332.2. Found: 332.

All other monomers in colorless liquid were prepared in a similar way. The spectra data are as follows.

*2.1.1.2. 2,5-Bis[(2-methyl butoxy)carbonyl]styrene (C5-2M).* $^1$H NMR ($\delta$, ppm): 0.92–1.87 (m, 18H, –CH($CH_3$)$CH_2CH_3$), 4.14–4.24 (m, 4H, –O–$CH_2$–), 5.38–5.44 (dd, 1H, =$CH_2$), 5.71–5.80 (dd, 1H, =$CH_2$), 7.27–7.45 (q, 1H, =CH–), 7.93–8.24 (m, 3H, Ar–H). IR ($cm^{-1}$): 1409, 1464, 1485, 1565 (Ar–), 1723 (C=O), 2878 (–$CH_3$, $\nu_s$), 2934 (–$CH_2$–), 2964 (–$CH_3$, $\nu_{as}$), and 3090 (–CH=$CH_2$). MS (*m*/*e*): Calcd. 332.2. Found: 332.

*2.1.1.3. 2,5-Bis[(3-methyl butoxy)carbonyl]styrene (C5-3M).* $^1$H NMR ($\delta$, ppm): 0.92–1.70 (m, 18H, –$CH_2$CH($CH_3$)$_2$), 4.33 (m, 4H, –O–$CH_2$–), 5.34–5.45 (dd, 1H, =$CH_2$), 5.71–5.80 (dd, 1H, =$CH_2$), 7.27–7.45 (q, 1H, =CH–), 7.91–8.24 (m, 3H, Ar–H). IR ($cm^{-1}$): 1409, 1465, 1485, 1564 (Ar–), 1722 (C=O), 2873 (–$CH_3$, $\nu_s$), 2932 (–$CH_2$–), 2960 (–$CH_3$, $\nu_{as}$), and 3090 (–CH=$CH_2$). MS (*m*/*e*): Calcd. 332.2. Found: 332.

*2.1.1.4. 2,5-Bis[(1,2-dimethyl propoxy)carbonyl]styrene (C5-1,2M).* $^1$H NMR ($CDCl_3$, $\delta$, ppm): 0.98–2.41 (m, 20H, –CH($CH_3$)CH($CH_3$)$_2$), 5.13 (m, 2H, –O–CH<), 5.39–5.45 (dd, 1H, =$CH_2$), 5.71–5.80 (dd, 1H, =$CH_2$), 7.27–7.45 (q, 1H, =CH–), 7.93–8.24 (m, 3H, Ar–H). IR ($cm^{-1}$): 1408, 1461, 1484, 1564 (Ar–), 1719 (C=O), 2877 (–$CH_3$, $\nu_s$), 2935 (–$CH_2$–), 2966 (–$CH_3$, $\nu_{as}$), and 3090 (–CH=$CH_2$). MS (*m*/*e*): Calcd. 332.2. Found: 332.

*2.1.1.5. 2,5-Bis[(1-methyl ethoxy)carbonyl]styrene (C3-1M).* $^1$H NMR ($\delta$, ppm): 1.36–1.41 (m, 12H, –$CH_3$), 5.26 (m, 2H, –CH<), 5.39–5.44 (dd, 1H, =$CH_2$), 5.71–5.80 (dd, 1H, =$CH_2$), 7.27–7.45 (q, 1H, =CH–), 7.83–8.22 (m, 3H, Ar–H). IR ($cm^{-1}$): 1408, 1458, 1484, 1564 (Ar–), 1719 (C =O), 2880 (–$CH_3$, $\nu_s$), 2974 (–$CH_3$, $\nu_{as}$), and 3090 (–CH=$CH_2$). MS (*m*/*e*): Calcd. 276.3. Found: 276.

*2.1.1.6. 2,5-Bis[(1-ethanyl propoxy)carbonyl]styrene (C5-1E).* $^1$H NMR ($\delta$, ppm): 0.92–1.00 (m, 12H, –$CH_3$), 1.69–1.76 (m, 8H, –$CH_2$–), 5.17 (m, 2H, –O–CH<), 5.40–5.45 (dd, 1H, =$CH_2$), 5.72–5.81 (dd, 1H, =$CH_2$), 7.27–7.45 (q, 1H, =CH–), 7.92–8.25 (m, 3H, Ar–H). IR ($cm^{-1}$): 1408, 1461, 1484, 1564 (Ar–), 1719 (C=O), 2880 (–$CH_3$, $\nu_s$), 2938 (–$CH_2$–), 2970 (–$CH_3$, $\nu_{as}$), and 3090 (–CH=$CH_2$). MS (*m*/*e*): Calcd. 332.2. Found: 332.

*2.2. Polymerization*

*2.2.1. Atom transfer radical polymerization (ATRP)*

The homopolymers PC3-1M with different molecular weights (MWs) were prepared at 90 °C in DMF. The initiating system was EBiB/CuBr/PMDETA (1:1:1, molar ratio). The polymerization was allowed to continue for 12 h. The molecular weight was adjusted by changing the molar ratio of monomer to initiator. In a typical run, C3-1M (0.88 g, 3.20 mmol), EBiB (0.04 g, 0.16 mmol), CuBr (0.02 mg, 0.16 mmol), PMDETA (0.03 mg, 0.16 mmol) and DMF (1.33 g) were introduced into a glass reaction tube. After three freeze–pump–thaw cycles, the tube was sealed off under vacuum and put into a thermostatic oil bath at 90 °C for 12 h. The tube was broken and the reaction mixture diluted with 15 mL of THF was let to pass through a short $Al_2O_3$ column. The crude product was obtained by adding the filtrate into 300 mL of methanol under rapid stirring and collection of precipitate by filtration. The operations of dissolution in THF and precipitation in methanol were repeated three times to remove the unreacted monomer. After drying at 50 °C under vacuum, 0.74 g of PC3-1M was obtained. The monomer conversion in weight was 84%. The properties of PC3-1M homopolymers used in this work are summarized in Table 1.

*2.2.2. Conventional radical polymerization*

The polymerization of the monomers was carried out in THF solution at 60 °C for 24 h using 0.3 mol% equiv AIBN as the initiator. The polymer was precipitated in and washed with large amount of methanol. The operations of dissolution in THF and precipitation in methanol were repeated three times. The characteristics of the homopolymers are summarized in Table 2.

*2.3. Measurement and characterization*

$^1$H NMR (300 MHz) spectra were recorded on a 300 MHz Varian Mercury Plus spectrometer at the ambient temperature using deuterated chloroform ($CDCl_3$) as the solvent and tetramethylsilane (TMS) as an internal standard. Mass spectra were obtained on a Micromass Finnigan MAT ZAB-HS mass spectrometer. Infrared

**Table 1**
Polymerization results of 2,5-bis[(1-methyl ethoxy)carbonyl]styrene (C3-1M).

| Sample ID | $M_{n,\,GPC}$[a] ($10^4$) | PDI[a] | $M_{n,\,GPC\text{-}LS}$[b] ($10^4$) | DP[b] | $T_g$[c] (°C) | Liquid crystallinity[d] | $T_{LC}$[d] (°C) |
|---|---|---|---|---|---|---|---|
| PC3-1M-1 | 0.59 | 1.09 | 0.88 | 32 | 62.9 | No | – |
| PC3-1M-2 | 0.99 | 1.14 | 1.42 | 51 | 69.5 | No | – |
| PC3-1M-3 | 1.45 | 1.14 | 2.17 | 79 | 76.0 | No | – |
| PC3-1M-4 | 2.08 | 1.14 | 2.95 | 107 | 80.4 | No | – |
| PC3-1M-5 | 2.60 | 1.13 | 3.49 | 126 | 80.3 | No | – |
| PC3-1M-6 | 2.85 | 1.11 | 3.72 | 135 | 80.5 | No[e] | –[e] |
| PC3-1M-7 | 3.48 | 1.10 | 4.49 | 162 | 83.3 | Yes | 160 |
| PC3-1M-8 | 7.58 | 1.33 | 12.9 | 467 | 85.0 | Yes | 146 |
| PC3-1M-9 | 10.15 | 1.31 | 18.33 | 663 | 89.8 | Yes | 140 |

[a] $M_n$: number-average molecular weight; $M_w$: weight-average molecular weight; PDI: polydispersity index ($M_w/M_n$), based on GPC measurements.
[b] $M_{n,\,GPC\text{-}LS}$: number-average molecular weight estimated by GPC-light scattering on line technique; DP: number-average polymerization degree calculated from $M_{n,\,GPC\text{-}LS}$.
[c] Glass-transition temperature obtained from the second heating DSC experiments.
[d] Determined by POM.
[e] No obvious birefringence can be observed under POM, but a diffraction peak in low 2$\theta$ angle region is identified on 1D WAXD pattern in the temperature range from 190 to 240 °C.

**Table 2**
Polymerization results of 2,5-bis(alkoxycarbonyl)styrene.

| Sample ID | $M_{n,\ GPC}$[a] ($10^5$) | PDI[a] | $T_g$ (°C) | Liquid crystallinity[b] | $T_{LC}$[c] (°C) | $T_d$[d] (°C) | $d$[e] (nm) |
|---|---|---|---|---|---|---|---|
| PC5-1M | 1.70 | 1.52 | 28 | Yes | 90 | 318 | 1.52 |
| PC5-2M | 1.97 | 1.43 | 9 | Yes | 50 | 347 | 1.53 |
| PC5-3M | 2.78 | 1.29 | 4 | Yes | 45 | 349 | 1.54 |
| PC5-1,2M | 1.72 | 1.47 | 81 | Yes | 106 | 317 | 1.54 |
| PC3-1M | 1.35 | 1.46 | 86 | Yes | 140 | 308 | 1.36 |
| PC5-1E | 1.93 | 1.42 | 52 | Yes | 60 | 308 | 1.55 |
| PC7-1P[10] | 0.10 | 2.2 | 10 | Yes | 40 | 308 | 1.58 |

[a] Based on GPC measurements.
[b] Determined by POM.
[c] Temperature at which mesophase was generated as characterized by POM observations.
[d] Temperature at which the weight loss of the polymers reached 5%.
[e] *d*-Spacing values of the polymers obtained at 220 °C by 1D WAXD.

(IR) spectra were recorded on a Nicolet Magna-IR 750 Fourier transform infrared spectrometer.

The number-average molecular weight ($M_{n,\ GPC}$), weight-average molecular weight ($M_{w,\ GPC}$), and polydispersity index (PDI, $M_{w,\ GPC}/M_{n,GPC}$) of the resultant polymers were estimated on a gel permeation chromatography (GPC) apparatus, which was equipped with a Waters 515 HPLC pump and a Waters 2410 refractive-index detector. Three Waters Styragel columns with a 10 μm bead size were connected in series. Their effective molecular weight ranges were 100–10 000 for Styragel HT2, 500–30 000 for Styragel HT3, and 5000–600 000 for Styragel HT4. The pore sizes were 50, 100, and 1000 nm for Styragels HT2–HT4, respectively. THF was used as the eluent at a flow rate of 1.0 mL min$^{-1}$ at 35 °C. Calibration was achieved against polystyrene standards.

The absolute number-average molecular weight ($M_{n,\ GPC\text{-}LS}$), weight-average molecular weight ($M_{w,\ GPC\text{-}LS}$), and number-average polymerization degree (DP, calculated from $M_{n,\ GPC\text{-}LS}$) of the polymers were characterized by the same GPC instrument mentioned above except that the Waters 2410 refractive-index detector was replaced with a Wyatt Technology DAWN HELEOS 18 angle (from 15 to 165°) light scattering detector using a Ga–As laser (658 nm, 40 mW). The concentration at each elution volume was determined with a Wyatt Optilab Rex interferometric differential refractometer (658 nm). The molecular weight data were calculated using Astra 5.1.6.0 software (Wyatt Technology). The refractive-index increment ($dn/dc$) of PC3-1M was estimated as 0.113 mL g$^{-1}$ in THF at room temperature by an Optilab Rex interferometric refractometer (Wyatt Technology) at the wavelength of 658 nm. The sample concentrations were 2.0, 4.0, 6.0, 8.0, 10.0, 12.0, and 14.0 mg mL$^{-1}$ctively. The refractometer was calibrated with aqueous NaCl solutions. All samples were dissolved in THF and stayed overnight before filtration for use through a 0.45 μm PTFE filter.

Thermogravimetric analyses (TGAs) were performed on a TA Q600 SDT instrument under nitrogen atmosphere at a heating rate of 20 °C min$^{-1}$ until 600 °C. The thermal transitions of the polymers were detected using TA DSC Q100 calorimeter in a temperature range of −50 to 150 °C. Samples with a typical mass of 5–8 mg were encapsulated in sealed aluminum pans. To readily observe glass transition, all the samples were cooled at a rate of 2 °C min$^{-1}$ from 150 to −50 °C first, and a subsequent heating was performed at a rate of 20 °C min$^{-1}$.

Mesophase textures were observed on a Leica DML polarized light optical microscope (POM) coupled with a Linkam TH-600PM Hot Stage. The images were taken with a camera. The samples were solution-cast films made on glass slides and the thickness of the films was kept at several microns.

One-dimensional wide-angle X-ray diffraction (1D WAXD) powder experiments were run on a Philips X'Pert Pro diffractometer with a 3 kW ceramic tube as the X-ray source (Cu Kα) and an X'celerator detector. The sample stage was set horizontally. The reflection peak positions were calibrated against silicon powder ($2\theta > 15°$) and silver behenate ($2\theta < 10°$). Background scattering was recorded and subtracted from the sample patterns. A temperature control unit (Paar Physica TCU 100) in conjunction with the diffractometer was used to investigate the structure evolutions as a function of temperature. The heating and cooling rates in the WAXD experiments were 10 °C min$^{-1}$.

Two-dimensional wide-angle X-ray diffraction (2D WAXD) fiber patterns were recorded on a Bruker D8 Discover diffractometer equipped with a general area detector diffraction system (GADDS) as a 2D detector, in a transmission mode at room temperature. Again, calibrations were made against silicon powder and silver behenate. Samples were mounted on the sample stage, and the point-focused X-ray beam was aligned either perpendicular or parallel to the mechanical shearing direction. Fibers were drawn at a stretching rate of about 1 m s$^{-1}$ at 200 °C and quenched to room temperature for measurements.

## 3. Results and discussion

### 3.1. Polymerization

Seven non-mesogenic vinyl monomers were synthesized as illustrated in Scheme 1. Among them, C3-1M and C7-1P were reported previously [10,39]. The other five compounds were new monomers. Their chemical structures and purities were characterized by $^1$H NMR, mass spectrometry and infrared techniques. To understand the molecular weight (MW) influence on the mesomorphic behaviors of the polymers, ATRP of C3-1M was carried out in DMF at 90 °C using the initiating system of EBiB/CuBr/PMDETA (1:1:1, molar ratio) to obtain the corresponding polymers with different MWs. As summarized in Table 1, the resultant polymers had $M_{n,\ GPC}$ ranging from $0.59 \times 10^4$ to $1.02 \times 10^5$ Da and PDI ranging from 1.09 to 1.33. All other monomers were polymerized via conventional radical polymerization to result in the corresponding polymers with high enough MWs (Table 2). For comparison, conventional radical polymerization of C3-1M was also carried out. All the polymers obtained had good solubilities in many common organic solvents such as acetone, chloroform, THF, DMF, dimethyl sulfoxide, and dichloromethane.

### 3.2. Thermal stability

TGA was employed to characterize the thermal stabilities of the polymers. As can be seen from Table 2, all the polymers were thermally stable and their 5% weight loss temperatures under nitrogen atmosphere were above 300 °C. Therefore, all the investigations were carried out below 280 °C under $N_2$ to rule out the possible influence of thermal decomposition on the liquid-crystalline phase of the polymers.

### 3.3. MW dependence of mesomorphic properties of PC3-1M

The thermotropic LC property of PC3-1M with $M_{n,\ GPC}$ of $8.6 \times 10^4$ Da has been studied by Yin et al. [39]. Based on DSC, POM, 1D and 2D WAXD results, this polymer was considered to form 2D $\Phi_H$ liquid-crystalline phase at the temperature well above its glass-transition temperature ($T_g$), while the MW dependence of phase structure and transition behaviors has not yet been discussed. Note that MW may influence the phase behavior in this system as well as in other MJLCPs [38]. We thus synthesized a series of PC3-1M samples with different MWs and narrow MW distributions and investigated their phase behaviors. As can be seen from Table 1, the

phase transition temperatures of PC3-1M show remarkable MW dependence. First, the $T_g$s observed in these samples increased with increasing $M_{n,\ GPC}$ and then leveled off when $M_{n,\ GPC}$ exceeded approximately $2.08 \times 10^4$ Da (Fig. 1). Second, the temperature of mesophase formation decreased with increasing $M_{n,\ GPC}$. Last, the LC phase formation was detected by both POM and WAXD. POM observations exhibited focal conic fanlike textures for PC3-1M only when $M_{n,\ GPC}$ exceeded $3.48 \times 10^4$ Da (Fig. 2). Fig. 3(a) illustrates a set of 1D WAXD patterns of as-cast sample PC3-1M-5 during the first heating in a $2\theta$ region of 2–30°. The scattering halo remained broad for the entire temperature range, indicating an amorphous structure. Fig. 3(b) and (c) illustrates the two sets of 1D WAXD patterns of sample PC3-1M-9 ($M_{n,\ GPC} = 10.15 \times 10^4$ Da) in a $2\theta$ region of 2–30° obtained during the first heating and the subsequent cooling course. At the first heating cycle, the low angle scattering halo increased its intensity dramatically at 140 °C and higher order diffractions were visible which could be maintained during the subsequent cooling cycle. The wide-angle scattering halo remained unchanged during both heating and cooling course, suggesting that no long-range ordered structure was formed on a scale of about 0.5 nm. The scattering vector ratio of the diffractions at the low angle region followed $1:\sqrt{3}:\sqrt{4}$, indicating that this sample possesses a hexagonal packing when heating to LC phase which was consistent with the conclusion reported previously [39]. Fig. 3(d) presents a set of 1D WAXD powder patterns in the low angle region for PC3-1M with various MWs obtained at 220 °C. The diffraction peaks had almost the same $2\theta$ value and higher order diffraction peaks in the low angle region were observed for the samples with $M_{n,\ GPC} \geq 2.85 \times 10^4$. Only the intensity of the low angle region diffraction peak increased with increasing $M_{n,\ GPC}$. Note that 1D WAXD revealed the generation of 2D $\Phi_H$ phase but

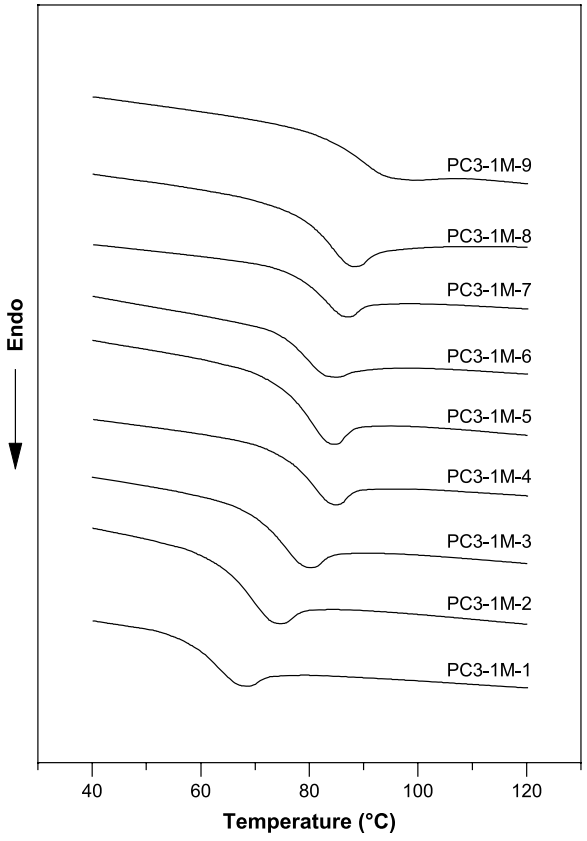


**Fig. 1.** Set of DSC curves of polymers PC3-1M during the second heating process at a heating rate of 20 °C min$^{-1}$ after cooling at 2 °C min$^{-1}$.

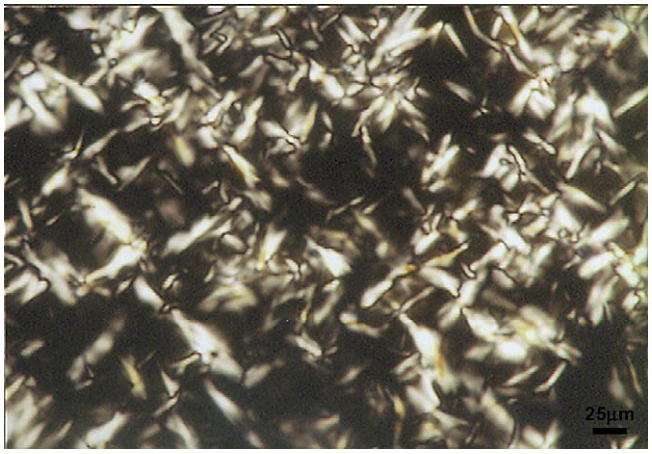


**Fig. 2.** POM photograph of PC3-1M-9 at 150 °C.

POM presented no birefringence for the sample with $M_{n,\ GPC}$ of $2.85 \times 10^4$ Da. To rule out the possible influence of MW, all the polymers studied below had $M_{n,\ GPC}$ larger than $1.35 \times 10^5$ Da.

### 3.4. Structure–property relationship

#### 3.4.1. Phase transitions

We first studied the variation in the terminal alkoxy groups on the $T_g$s of the polymers. To make the glass transition more evident and eliminate the complex thermal history of samples generated during drying, thermal hysteresis was introduced by slowly cooling the sample from high temperature followed by fast heating. The $T_g$s were determined using the second DSC heating traces. Fig. 4 shows second heating DSC thermograms of the polymers recorded at a rate of 20 °C min$^{-1}$. All the DSC curves were featureless except for glass transitions. The $T_g$s of the polymers gradually decreased for PC5-*n*M as the branching point was increasingly farther away from the site connecting with ester bond. This indicated that moving the methyl group away from the ester bond increased the plasticization of the polymer backbone. As graft density changed from one to two, the $T_g$ of PC5-1,2M abruptly increased to 81.3 °C due to the enhanced rigidity of the polymer backbone. For the series of PCm-1R, this kind of polymers had only one phenylene group connecting with two double-swallow tailed (Y-shaped) groups via an ester linkage in each side-chain template. When the substituted group changed from C3-1M to C7-1P, the $T_g$ of the polymer remarkably decreased. Two competitive factors influencing the $T_g$ of the polymers may exist. On the one hand, it makes the $T_g$ of the polymers to increase due to the enhanced rigidity of the polymer backbones as the size of the substituent groups becomes larger. On the other hand, the $T_g$ of the polymers decreases because an increasing length of the alkoxy tails leads to the decreased packing density imposed by the enhanced internal plasticization. In the current study, the latter was dominant.

#### 3.4.2. Morphologies

According to the previous report [39], one interesting property of PC3-1M was that it melted into isotropic fluid first upon heating and then formed mesophase at the temperature well above its $T_g$. Liquid-crystalline phases of the polymers obtained were first studied by POM observation. At room temperature, all the polymers exhibited only very weak birefringence under POM, presumably because of the existence of some ordered arrangement of the polymer chain that formed during precipitation. The lack of crystallinity of these and other homologous MJLCPs indicated that the

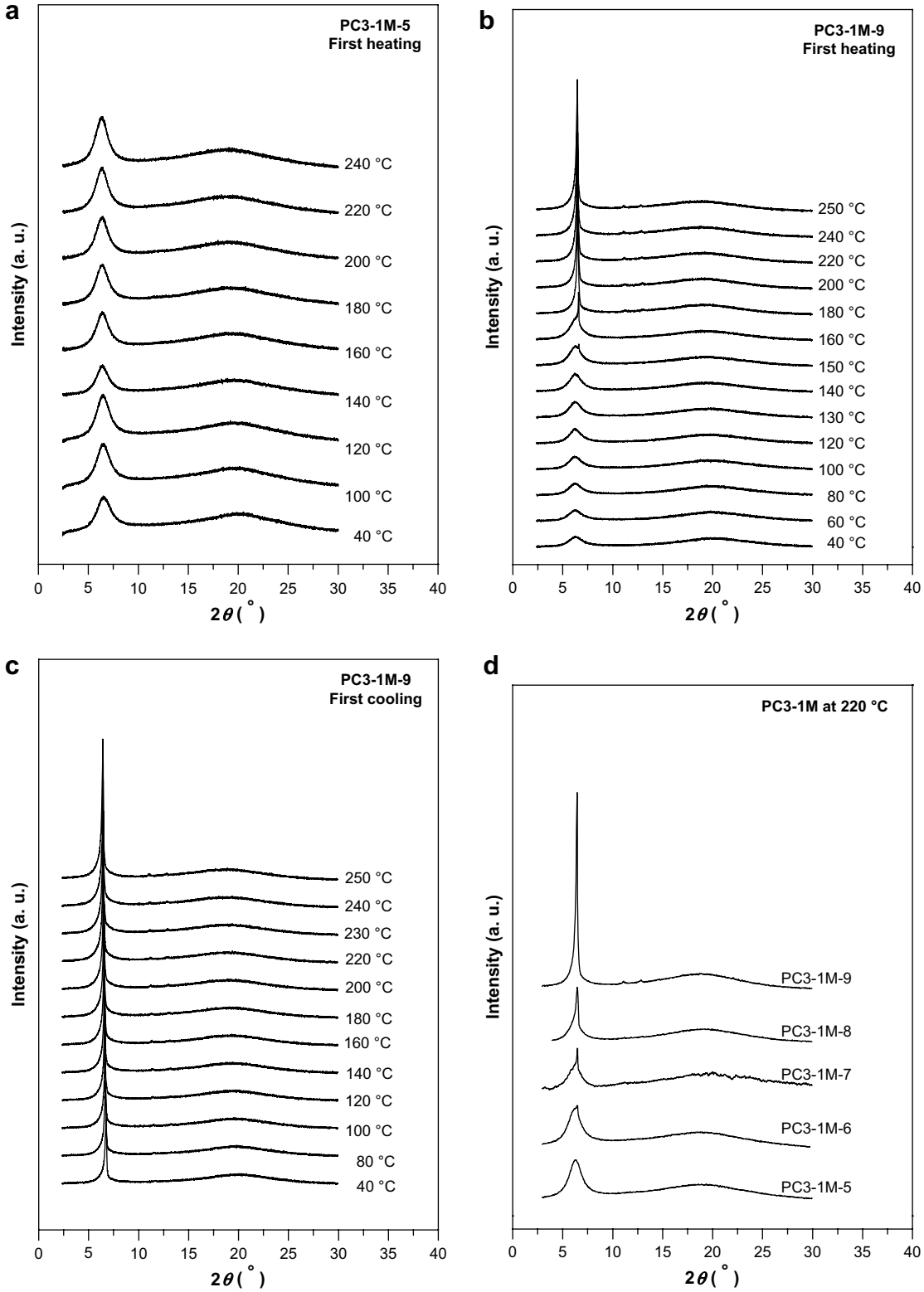


**Fig. 3.** 1D WAXD diffraction powder patterns in a $2\theta$ region of 2–30° for samples PC3-1M-5 during the first heating (a), PC3-1M-9 during the first heating (b), the subsequent cooling course (c) and a set of the 1D WAXD patterns at 220 °C for PC3-1M with different MWs.

bulky side groups hindered the crystallization of these polymers [42]. Obvious birefringence was observed when the samples were heated to a certain temperature ($T_{LC}$) higher than $T_g$, as shown in Table 2. The temperatures of entering LC phase ($T_{LC}$s) of the polymers decreased both for PC5-*n*M as the branching point was increasingly farther away from the site connecting with ester bond and for PCm-1R when the substituted group changed from C3-1M to C7-1P. The $T_{LC}$ abruptly increased to 106 °C for PC5-1,2M as the

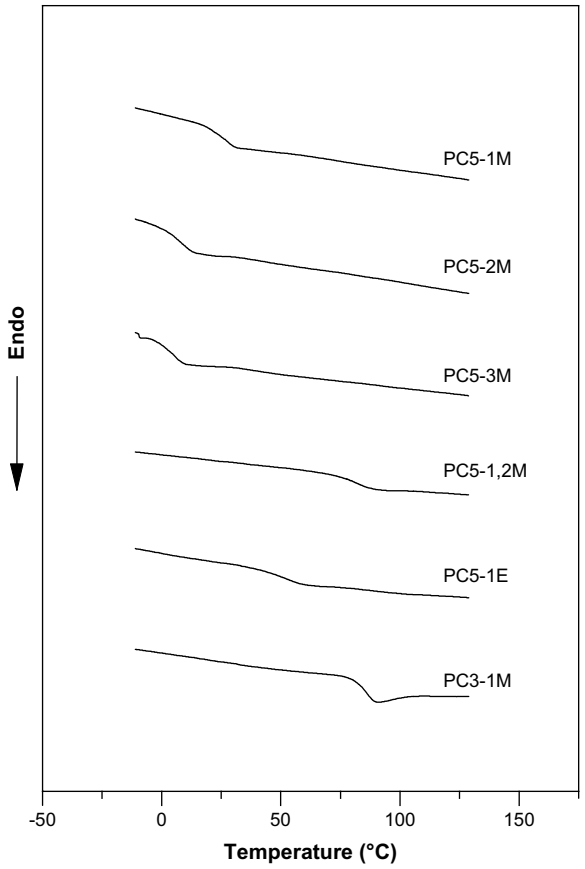


**Fig. 4.** Set of DSC curves of poly[2,5-bis(alkoxycarbonyl)styrenes] during the second heating process at a heating rate of 20 °C min$^{-1}$ after cooling at 2 °C min$^{-1}$.

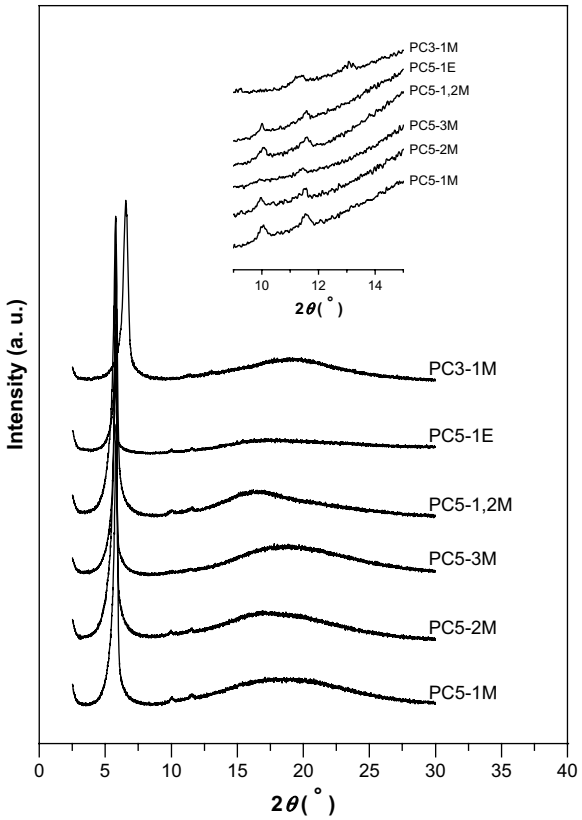


**Fig. 6.** 1D WAXD patterns in a 2$\theta$ region of 2–30° of homopolymers at 220 °C. The inset is the enlarged 2$\theta$ region of 8–18°.

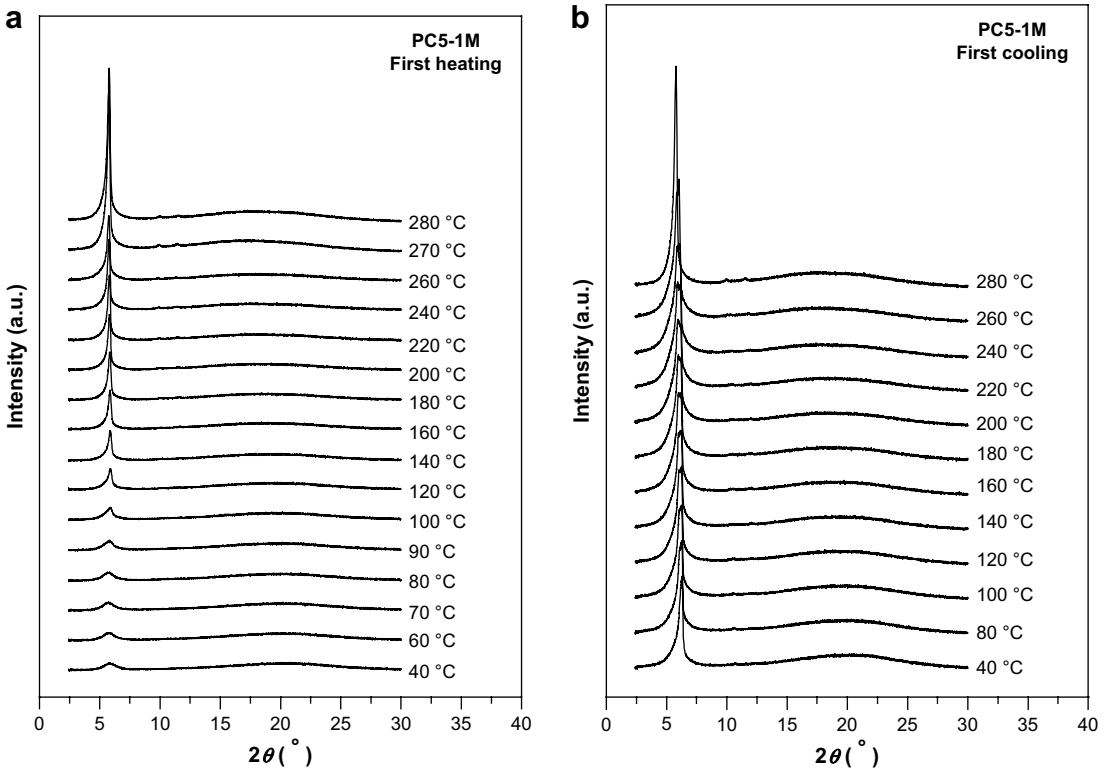


**Fig. 5.** 1D WAXD powder patterns in a 2$\theta$ region of 2–30° for polymer PC5-1M during the first heating (a) and the subsequent cooling course (b).

**Table 3**
1D WAXD results of the polymers at 220 °C.

| Sample ID | $2\theta$ (°) | $d$ (nm) | $q$-Ratios |
|---|---|---|---|
| PC5-1M | 5.78, 10.0, 11.5 | 1.52, 0.887, 0.769 | 1:√3:√4 |
| PC5-2M | 5.76, 9.97, 11.5 | 1.53, 0.892, 0.775 | 1:√3:√4 |
| PC5-3M | 5.73, 9.86, 11.4 | 1.54, 0.896, 0.775 | 1:√3:√4 |
| PC5-1,2M | 5.75, 10.0, 11.5 | 1.54, 0.887, 0.769 | 1:√3:√4 |
| PC3-1M | 6.49, 11.2, 12.9 | 1.36, 0.789, 0.685 | 1:√3:√4 |
| PC5-1E | 5.69, 9.91, 11.5 | 1.55, 0.891, 0.769 | 1:√3:√4 |
| PC7-1P[10] | 5.60, 9.64, 11.1 | 1.58, 0.917, 0.795 | 1:√3:√4 |

branching site changed from one to two. No obvious extinction of the birefringence could be observed before the polymers decomposed (onset temperature > 300 °C). POM observations exhibited focal conic fanlike textures (PC3-1M and PC5-1M) or star-shaped texture for solution-cast films of the polymers isothermally annealed at 150 °C for several minutes. However, the poor mobility of the polymer chain prevented the development of a characteristic texture. As a result, the LC phase could not be identified by texture investigation only.

### 3.4.3. Structures

To identify the ordered structures developed in these polymers, 1D WAXD experiments were carried out with the solution-cast samples. Fig. 5 illustrates the temperature-variable 1D WAXD patterns of PC5-1M in the $2\theta$ region from 2.5° to 30°, which were recorded during the first heating and the subsequent cooling runs, respectively. The $T_g$ of the polymer was 28 °C. A low angle broad scattering halo was observed at the starting test temperature, i.e., 40 °C, which was higher than the $T_g$ of the polymer. The scattering halo was asymmetric and could be deconvoluted into one broad halo and one narrow reflection peak at 100 °C. The intensity of the halo increased gradually with an increase in the temperature and developed into a sharp peak ($2\theta = 5.8°$, with a $d$-spacing value of 1.52 nm). This indicated the ordered structures on the nanometer scale developed. It was consistent with the POM result. Raising temperature led to a substantial enhancement in the intensity of the reflection peak, and the peak shifted continuously and slightly to lower $2\theta$ value due to the thermal expansion. Second-order diffractions were visible (the enlarged curve of polymers in Fig. 6, the scattering vector ratio of the diffractions followed 1:√3:√4), indicating a long-range ordered hexagonal lattice. In the wide-angle region of $2\theta > 12°$, only an amorphous halo around 20° could be recognized. This reflected that no long-range ordered structure formed via molecular packing was detected on a scale of 0.5 nm over the entire temperature region studied. After the first heating to 280 °C, a cooling WAXD experiment of the polymer was carried out, as shown in part b of Fig. 5. The evolved reflection peak at $2\theta = 5.8°$ remained permanently, but the scattering intensity became weaker with decreasing temperature. This reflected that the electron density difference generating this

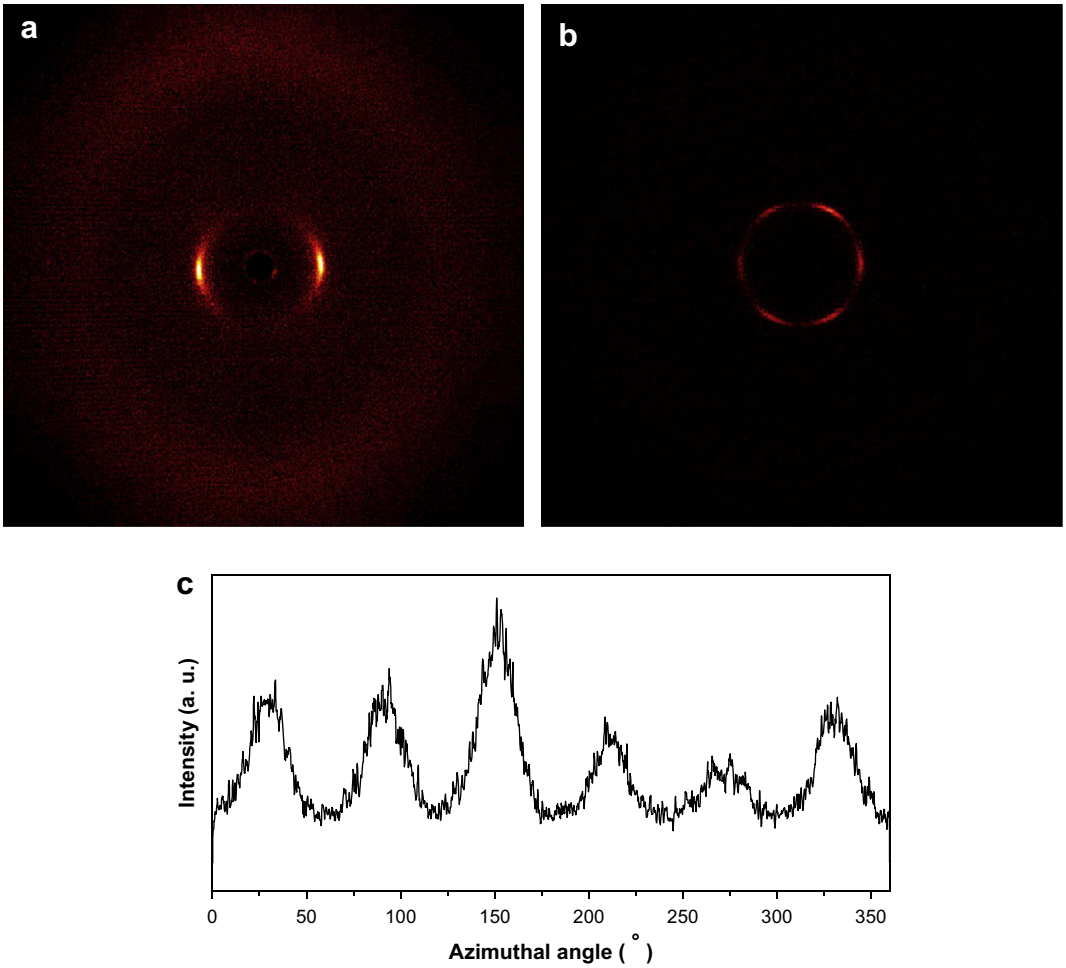


**Fig. 7.** 2D WAXD fiber patterns of PC5-1M. The X-ray incident beam was perpendicular (a) and parallel (b) to the fiber axis, and (c) the azimuthal scanning data of the low $2\theta$ region diffraction.

scattering on the nanometer scale decreased when the temperature was lowered [38]. Furthermore, the 1D WAXD experiments of other polymers were also performed (Fig. 6), and similar phenomena to that of PC5-1M were observed. Table 3 depicts the *d*-spacing values measured from sets of 1D WAXD patterns of the homopolymers at 220 °C. The *d*-spacing value of mesophase increased for PC5-*n*M as the methyl substituent was away from connecting phenyl ring. In the case of polymers with Y-shaped alkyl groups, the bigger the side groups, the larger the *d*-spacing values. This kind of MJLCPs containing flexible and branched side substituted group based on 2,5-bis(alkoxycarbonyl)styrene were apt to form hexagonal columnar liquid-crystalline phase by fine-tuning the graft point and shape of the side groups.

To further study structural dimensionality, 2D WAXD experiments on the oriented samples were carried out by aligning the X-ray incident beam along different directions. Part a of Fig. 7 is 2D WAXD pattern at room temperature of the oriented sample PC5-1M with the X-ray incident beam perpendicular to the fiber axis. In the figure, the fiber axis is parallel to the meridian direction. A pair of strong diffraction arcs could be seen on the equator at $2\theta = 5.8^\circ$ (*d*-spacing of 1.52 nm) which was consistent with the 1D WAXD results, indicating that the ordered structures had developed along the direction perpendicular to the fiber axis on the nanometer scale. On the other hand, scattering halos in the high $2\theta$ region were more or less centered on the meridian with rather broad azimuthal distributions. This revealed that only short-range order existed along the fiber direction. Fig. 7(b) presents a six-fold symmetry of the (100) diffractions in the same sample when the X-ray beam was parallel to the shear direction. Note that the columns were aligned along the shear direction. The corresponding azimuthal intensity profile which exhibited six maxima with an angle of 60° between two adjacent diffraction maxima is shown in Fig. 7(c). Therefore, the 2D WAXD results confirmed that PC5-1M exhibited a 2D $\Phi_H$ phase in which the building blocks involved entire molecules having relatively extended conformation. The 2D WAXD experiment results of other polymers were similar to that of PC5-1M.

Combining 1D and 2D WAXD results with PLM observations, all the polymers showed stable 2D $\Phi_H$ liquid-crystalline phase at high temperature and remained upon cooling to room temperature.

## 4. Conclusions

Two-dimensional hexagonal columnar liquid-crystalline phase (2D $\Phi_H$) was generated in a series of vinyl polymers, poly[2,5-bis(alkoxycarbonyl)styrene], which contained no traditional mesogenic unit. The polymers distinguished other LCPs by the fact that they first became isotropic melt upon heating and then ordered into 2D $\Phi_H$ phase. It was considered that the direct linking of dialkyl terephthalate via waist position to polymer backbone at every second carbon atom played an important role in the mesophase formation, i.e., by self-assembly of main chain and side groups, macromolecules behaved as supramolecular cylinders with high population of side groups as the periphery and generated orientational ordered packing. The phase transition temperature and the mesomorphic structure size were readily tuned by subtle variation of alkoxy terminals, which provided a facile way to tailor the structure and property of the polymers in terms of application.

## Acknowledgment

The financial support from the National Natural Science Foundation of China (Grants 20674001 and 20134010) and the National Distinguished Young Scholar Fund (Grant 20325415) is gratefully acknowledged.

## References

[1] Percec V, Pugh C. In: McArdle CB, editor. Side chain liquid crystal polymers. New York: Chapman and Hall; 1989.
[2] Magagnini PL, Marchetti A, Matera F, Pizzirani G, Turchi G. Eur Polym J 1974; 10:585.
[3] Hessel F, Finkelmann H. Polym Bull 1985;14:375.
[4] Gray GW, Hill JS, Lacey D. Mol Cryst Liq Cryst 1990;7:47.
[5] (a) Finkelmann H, Ringsdorf H, Wendorff HJ. Makromol Chem 1978;179:273; (b) Finkelmann H, Wendorff HJ. Structure of nematic side chain polymers. In: Blumstein A, editor. Polymeric liquid crystals. New York: Plenum; 1985. p. 295.
[6] Zhou QF, Li HM, Feng XD. International conference on liquid crystal polymers. Bordeaux, France; 1987. p. 401.
[7] Zhou QF, Li HM, Feng XD. Macromolecules 1987;20:233.
[8] Zhou QF, Zhu XL, Wen ZQ. Macromolecules 1989;22:491.
[9] Zhu X, Yang Q, Zhou QF. Chin J Polym Sci 1992;10:187.
[10] Tu HL, Wan XH, Liu YX, Chen XF, Zhang D, Zhou QF, et al. Macromolecules 2000;33:6315.
[11] Hardouin F, Mery S, Achard MF, Noirez L, Keller P. J Phys II 1991;1:511.
[12] Hardouin F, Leroux N, Mery S, Noirez L. J Phys II 1992;2:271.
[13] Leroux N, Keller P, Achard MF, Noirez L, Hardouin F. J Phys II 1993;3:1289.
[14] Lecommandoux S, Achard MF, Hardouin F, Brulet A, Cotton JP. Liq Cryst 1997;22:549.
[15] Cherodian A, Hughes M, Noirez L, Hardouin F. Liq Cryst 1994;16:421.
[16] Cherodian AS, Hughes NJ, Richardson RM, Lee MSK, Gray GW. Liq Cryst 1993;14:1667.
[17] Gray GW, Hill JS, Lacey D. Mol Cryst Liq Cryst 1991;197:43.
[18] Xu GZ, Wu W, Shen DY, Hou JN, Zhang SF, Xu M, et al. Polymer 1993;34:1818.
[19] Xu GZ, Wu W, Xu M, Zhou QF. J Polym Sci Part B Polym Phys 1993;31:229.
[20] Wan XH, Zhang F, Wu PQ, Zhang D, Feng XD, Zhou QF. Macromol Symp 1995;96:207.
[21] Pugh C, Shao J, Ge JJ, Cheng SZD. Macromolecules 1998;31:1779.
[22] Gopalan P, Andruzzi L, Li XF, Ober CK. Macromol Chem Phys 2002;203:1573.
[23] Gopalan P, Zhang YM, Li XF, Wiesner U, Ober CK. Macromolecules 2003;36:3357.
[24] Pragliola S, Ober CK, Mather PT, Jeon HG. Macromol Chem Phys 1999;200:2338.
[25] Zhang D, Zhou QF, Ma YG, Wan XH, Feng XD. Polym Adv Technol 1997;8:227.
[26] Liu MH, Keller P, Grelet E, Philippe A. Macromol Chem Phys 2002;203:619.
[27] Zhou QF, Wan XH, Zhu XL, Zhang F, Feng XD. Mol Cryst Liq Cryst 1993;231:107.
[28] Wan XH, Zhou QF, Zhang D, Zhang Y, Feng XD. Chem J Chin Univ 1998;19:1507.
[29] Zhou QF, Wan XH, Zhang D, Feng XD. In: Isayev AI, Kyu T, Cheng SZD, editors. Liquid crystalline polymer systems: technological advances. ACS Symposium Series 632. Washington, DC: American Chemical Society; 1996. p. 344.
[30] Zhang D, Liu YX, Wan XH, Zhou QF. Macromolecules 1999;32:4494.
[31] Zhang D, Liu YX, Wan XH, Zhou QF. Macromolecules 1999;32:5183.
[32] Yu ZN, Tu HL, Wan XH, Chen XF, Zhou QF. Mol Cryst Liq Cryst 2003;391:41.
[33] Yu ZN, Tu HL, Wan XH, Chen XF, Zhou QF. J Polym Sci Part A Polym Chem 2003;41:1454.
[34] Tu HL, Yu ZN, Wan XH, Li L, Sun L, Chen XF, et al. Macromol Symp 2001;164:347.
[35] Tu HL, Yu ZN, Wan XH, Chen XF, Zhou QF. Chem J Chin Univ 2000;21:985.
[36] Zhu ZG, Zhi JG, Liu AH, Cui JX, Tang H, Qiao WQ, et al. J Polym Sci Part A Polym Chem 2007;45:830.
[37] Li CY, Tenneti KK, Zhang D, Zhang HL, Wan XH, Chen EQ, et al. Macromolecules 2004;37:2854.
[38] Ye C, Zhang HL, Huang Y, Chen EQ, Lu YL, Shen DY, et al. Macromolecules 2004;37:7188.
[39] Yin XY, Ye C, Ma X, Chen EQ, Qi XY, Duan XF, et al. J Am Chem Soc 2003;125:6854.
[40] Zhao YF, Fan XH, Wan XH, Chen XF, Yi Y, Wang LS, et al. Macromolecules 2006;39:948.
[41] Chen XF, Tenneti KK, Li CY, Bai YW, Zhou R, Wan XH, et al. Macromolecules 2006;39:517.
[42] Kim GH, Pugh C, Cheng SZD. Macromolecules 2000;33:8983.
[43] Arehart SV, Pugh C. J Am Chem Soc 1997;119:3027–37.
[44] Pugh C, Bae JY, Dharia J, Ge JJ, Cheng SZD. Macromolecules 1998;31:5188.
[45] Small AC, Pugh C. Macromolecules 2002;35:2105.
[46] Chen S, Gao LC. Macromolecules 2007;40:5718.
[47] Chai CP, Zhu XQ, Wang P, Ren MQ, Chen XF, Xu YD, et al. Macromolecules 2007;40:9361.
[48] Tsubakihara S, Nakamura A, Yasuniwa M. Polym J 1996;28:489.
[49] Desper C, Schneider N. Macromolecules 1976;9:424.
[50] Tur D, Provotorova N, Vinogradova S, Bakhmutov V, Galakhov M, Zhukov V, et al. Makromol Chem 1991;192:1905.
[51] Papkov V, Ilina M, Zhukov V, Tsvankin D, Tur D. Macromolecules 1992;25:2033.
[52] Molenberg A, Möller M, Sautter E. Prog Polym Sci 1997;22:1133.
[53] Molenberg A, Siffrin S, Möller M, Boileau S, Teyssie D. Macromol Symp 1996;102:199.
[54] Molenberg A, Klok H, Möller M, Boileau S, TeyssiC D. Macromolecules 1997;30:792.
[55] Molenberg A, Möller M. Macromolecules 1997;30:8332.
[56] Molenberg A, Möller M, Pieper Thomas. Macromol Chem Phys 1998;199:299.